Journal of Inorganic Biochemistry 206 (2020) 111013

Contents lists available at ScienceDirect

Journal of Inorganic Biochemistry

journal homepage: www.elsevier.com/locate/jinorgbio

Modulation of the catalytic activity of a metallonuclease by tagging with oligohistidine

Heba A.H. Abd Elhameed[a,1], Bálint Hajdu[a], Attila Jancsó[a], Albert Kéri[a], Gábor Galbács[a], Éva Hunyadi-Gulyás[b], Béla Gyurcsik[a,*]

[a] Department of Inorganic and Analytical Chemistry, University of Szeged, Dóm tér 7, H-6720 Szeged, Hungary
[b] Laboratory of Proteomics Research, Biological Research Centre, Temesvári krt. 62, H-6726 Szeged, Hungary

ARTICLE INFO

Keywords:
NColE7 nuclease
Zinc(II)
DNA hydrolysis
Mass spectrometry
6 × His tag

ABSTRACT

Peptide tags are extensively used for affinity purification of proteins. In an optimal case, these tags can be completely removed from the purified protein by a specific protease mediated hydrolysis. However, the interactions of these tags with the target protein may also be utilized for the modulation of the protein function. Here we show that the C-terminal hexahistidine (6 × His) tag can influence the catalytic activity of the nuclease domain of the Colicin E7 metallonuclease (NColE7) used by *E. coli* to kill competing bacteria under stress conditions. This enzyme non-specifically cleaves the DNA that results in cytotoxicity. We have successfully cloned the genes of NColE7 protein and its R447G mutant into a modified pET-21a DNA vector fusing the affinity tag to the protein upon expression, which would be otherwise not possible in the absence of the gene of the Im7 inhibitory protein. This reflects the inhibitory effect of the 6 × His fusion tag on the nuclease activity, which proved to be a complex process via both coordinative and non-specific steric interactions. The modulatory effect of Zn^{2+} ion was observed in the catalytic activity experiments. The DNA cleavage ability of the 6 × His tagged enzyme was first enhanced by an increase of metal ion concentration, while high excess of Zn^{2+} ions caused a lower rate of the DNA cleavage. Modelling of the coordinative effect of the fusion tag by external chelators suggested ternary complex formation instead of removal of the metal ion from the active center.

1. Introduction

Recently we reported about a new strategy of protein purification by a C-terminal metal ion affinity fusion tag, using a new gene carrier plasmid DNA. The self-eliminating *Bsm*BI restriction enzyme sites allowed for the insertion of the gene of the target protein between the atg "start" codon and the nucleotide sequence encoding for the (Ser/Thr)-X-His-X ((S/T)XHX) segment instead of the stop codon [1]. The latter sequence can be hydrolyzed by Ni(II) ions at the N-terminus of the Ser/Thr amino acid [2–7], and in this way, any kind of C-terminal affinity tags can be easily removed from the expressed protein without leaving any additional amino acids at the termini of the native protein sequence. Such peptide bond cleavage initiated by Ni(II) ions has already found application in the affinity tag removal from fusion proteins [8–10].

Oligohistidine fusion sequences are applied in metal ion affinity chromatography due to their metal complexing ability through the multiple imidazoles offered by the amino acid side chains. Although it was shown that the affinity tags do not significantly affect the crystal structures [11], they may influence the folding and thermal stability of the protein, and/or its function through non-specific steric interactions. Such effects have been observed in various proteins, exemplified by refs. 12–23. His tag incorporation in myoglobin reduced the dynamics of the protein motion, as demonstrated by the fluctuations of the CO vibrational frequency [12]. The N-terminal His tag of the trimeric cytokine tumor necrosis factor alpha (TNFα) led to a decrease of its cytotoxicity on the L-929 cell line by an order of magnitude, while the removal of the tag re-established its normal biological activity [13]. The incorporation of the C-terminal hexahistidine tag into tropinone reductase showed steric and electrostatic interference with the active site resulting in impaired K_M value for nitrogen-containing substrates [14]. The His tag may also inhibit the binding of a peptide substrate by competition [24].

Even more importantly, the oligohistidine sequences may coordinate to metal ions [25–29]. This property may be utilized by labelling proteins with metal complexes [30,31] or nanoparticles [32,33],

* Corresponding author.
E-mail address: gyurcsik@chem.u-szeged.hu (B. Gyurcsik).
[1] Presently PhD student at University of Szeged. Home affiliation: Department of Chemistry, Faculty of Science, Zagazig University, Egypt.

https://doi.org/10.1016/j.jinorgbio.2020.111013
Received 30 September 2019; Received in revised form 23 January 2020; Accepted 27 January 2020
Available online 01 February 2020

NColE7-6×His KRNKPGKATGKGKPVNNKWLNNAGKDLGSPVPDRIANKLRDKEFKSFDDFRKKFWE
EVSKDPELSKQFSRNNNDRMKVGKAPKTRTQDVSGKRTSFELHHEKPISQNGGVYDMDNISVVTPKRHIDIHRGK
SRHSEFELVDKLAAALEHHHHHH

Scheme 1. The amino acid sequence of the NColE7-6 × His protein. The arginine (R447) amino acid highlighted by the grey character background close to the N-terminus was mutated to glycine (R447G mutation) to yield the KGNK-6 × His protein. H544, H569 and H573 metal ion-binding histidines are underlined in the HNH motif (red characters), and the general base H545 histidine is underlined and also highlighted by the grey character background. The fusion sequence is in italic, in which the SRHS nickel(II)-sensitive motif and the hexahistidine function is underlined. The numbering of the amino acids is based on the original Colicin E7 amino acid sequence.

by immobilization on membranes [34] or metal ion derivatized surfaces [35], as well as by introducing new functions [36,37]. The metal ions bound within the metalloproteins may also be targeted by the oligohistidine coordination. Since metal ions play a role in the folding, stabilization of the structure, catalytic activity and/or regulation of the function of various metalloproteins, all these properties may be influenced by the presence of the affinity tag. Such interactions are much less discussed in the literature. As an example, the decrease in the release of iron from recombinant human serum transferrin was observed in the presence of C-terminal His tag most likely due to the stabilization of the metal ion by the complexation with the tag [38].

These findings highlight the possibility of tailoring the properties of a selected metalloprotein by applying an oligohistidine fusion sequence. In the present paper we show, how the C-terminal hexahistidine fusion tag can modulate the nuclease activity of the C-terminal nuclease domain of the Colicin E7 metalloprotein (NColE7) via both non-specific and coordinative interactions. To investigate this phenomenon we have synthesized the genes of the NColE7-6 × His protein (Scheme 1) and its selected mutants to express the proteins within *E. coli* cells. Whenever it was possible, we also purified the protein, for further characterization of its solution structure, metal ion-binding and catalytic activity.

2. Experimental

2.1. Strains and media

Mach1 and DH5α competent *E. coli* cells were used for cloning the recombinant DNA and BL21(DE3) competent *E. coli* cells for protein expression. Bacteria were grown in lysogeny broth (LB) medium [39] containing ampicillin in 0.1 mg/mL final concentration (amp+) at 37 °C. We checked the effect of NColE7 and its mutants on bacterial colony formation on ampicillin containing LB(amp+) agar plates.

2.2. Plasmid construction

The new pET-21a*-SRHS plasmid DNA was modified from the pET-21a commercial DNA vector. The new cloning site includes two *Bsm*BI restriction sites, the codes of SRHS (allowing to cleave the fusion tag in the expressed protein by Ni(II), which can induce peptide-bond hydrolysis at the SRH sensitive sequence), a linker and a 6 × His tag sequence. The genes of NColE7 (the original pQE70-NColE7/Im7 plasmid [40] was kindly provided by prof. Kin-Fu Chak from Institute of Biochemistry, National Yang-Ming University, Taipei, Taiwan, Republic of China) and its less active R447G mutant protein (further denoted as KGNK) were cloned separately to yield the new protein expression DNA constructs: pET-21a*-NColE7-SRHS and pET-21a*-KGNK-SRHS, expressing NColE7-6 × His (Scheme 1) and KGNK-6 × His proteins, respectively. The codon of the histidine amino acid of the SRHS motif was further mutated via a modified QuikChange™ protocol within both the pET-21a*-NColE7-SRHS and pET-21a*-KGNK-SRHS plasmids resulting the pET-21a*-NColE7-SRQS and pET-21a*-KGNK-SRQS plasmids including a histidine (H) to glutamine (Q) mutation. We also inserted a new oligonucleotide sequence between the SRQS and 6 × His tag codes of the pET-21a*-NColE7-SRQS and pET-21a*-KGNK-SRQS plasmids to obtain new plasmids, which were expected to express proteins with a non-coordinating C-terminal extension instead of the 6 × His sequence. The construction of the above plasmids and the sequences of expected proteins are described in detail in the Supplementary material. The ligated plasmids, multiplied by competent *E. coli* cells were purified from the bacteria by EZ-spin column plasmid DNA kit (Bio Basic Inc., Canada). The nucleotide sequences of the plasmids were verified by the standard sequencing procedure.

2.3. Protein expression and purification

The KGNK-6 × His protein was expressed by the same method described in our previous article [1] with changes during the purification procedure since the protein was eluted here from the Ni(II)-nitrilotriacetic acid (NTA) resin without cleaving the 6 × His affinity tag. The protein was expressed in BL21 (DE3) *E. coli* cells from the pET-21a*-KGNK-SRHS expression plasmid by growing the bacteria first in 5 mL LB(amp+) media for ~6 h at 37 °C until the optical density reached 0.6–1.0. This preculture was transferred into 250 mL LB(amp+) medium (containing 0.1 mg/mL ampicillin) and incubated further for ~4 h at 37 °C. The protein expression was induced by 150 μL isopropyl β-D-1-thiogalactopyranoside (IPTG; 200 mg/mL stock diluted to ~0.5 mM final concentration) when the optical density at 600 nm (OD_{600}) reached 0.9–1.0. After incubation for 3 h at 37 °C the cells were collected by centrifugation at 4 °C, 4000 ×*g* for 15 min. The cells were resuspended in 10 mL 1 × binding buffer containing 500 mM NaCl, 20 mM tris(hydroxymethyl)aminomethane hydrochloride (Tris-HCl; pH 7.9), and 5 mM imidazole. The cells were lysed by ultrasonication with a 50% amplitude setting for 6 × 30 s using a VCX 130 PB (130 W) ultrasonic processor equipped with a 129 mm long and 13 mm diameter titanium probe and the extract was centrifuged at 4000 ×*g* for 35 min at 4 °C. After these preparatory steps, the KGNK-6 × His protein was purified in batch type nickel-affinity chromatography. The sample was filtered and loaded onto a Novagen His•Bind® resin preequilibrated with 1 × binding buffer and rotated for 1 h at 4 °C. The bound protein was washed 5 times with 2 × bed volume wash buffer (20 mM Tris-HCl pH 7.9, 500 mM NaCl) containing increasing amounts of imidazole (0–100 mM). After the washing steps, the protein was eluted from the resin by using 0.25 × bed volume 1 × elution buffer (20 mM Tris-HCl, pH 7.9, 500 mM NaCl, 1 M imidazole). The protein solution was buffer-exchanged using Amicon Ultra 0.5 mL centrifugal filters with 3 kDa molecular weight cut-off and stored in 20 mM 4-(2-hydroxyethyl)-1-piperazineethanesulfonic acid (HEPES, pH 7.7). Protein samples obtained during the purification were analysed by tricine modified sodium dodecyl sulfate -polyacrylamide gel electrophoresis (SDS-PAGE) using polyacrylamide gels prepared according to the protocol described in ref. [41]. The bands were visualized by Coomassie Brilliant Blue staining. Precision Plus Protein™ All Blue prestained protein standard (BioRad) was run as a marker for comparison in each electrophoresis experiment. The KGNK and NColE7 proteins were prepared as previously described [42].

2.4. Circular dichroism (CD) spectroscopy

Circular dichroism spectra were recorded on a Jasco J-815

spectropolarimeter while synchrotron radiation circular dichroism (SRCD) spectra were acquired at the CD1 beamline of the storage ring ASTRID at the ISA Centre for Storage Ring Facilities Aarhus, Aarhus University, Denmark [43,44]. Camphor-sulfonic acid served as a calibration material for the instrument. All spectra were recorded using 1 nm steps and a dwell time of 2 s, using quartz cells (SUPRASIL, Hellma GmbH, Germany) with a 0.1 mm optical length, in the wavelength range of 180–300 nm. Prior to the measurements, the protein solutions were dialyzed against a 10 mM HEPES, pH 8.2 buffer. Spectra were baseline-corrected by using the spectrum of water or buffer.

2.5. Inductively coupled plasma mass spectrometry experiments

An Agilent 7700× inductively coupled plasma mass spectrometer (ICP-MS) was used for the quantitative measurement of total zinc concentrations. The sample introduction system consisted of an Agilent I-AS autosampler and a Micro Mist pneumatic nebulizer equipped with a Peltier-cooled Scott-type spray chamber. The sample uptake rate was 400 μL/min. The ICP plasma and interface parameters were set up as follows. Radio frequency forward power: 1550 W, plasma gas flow rate: 15.0 L/min, carrier gas flow rate: 1.05 L/min, sampling depth: 10.0 mm. In order to avoid possible spectral interferences, the measurements were performed in He mode of the collision cell. Measurements were carried out by monitoring the signal of the ^{66}Zn isotope. ICP-MS tuning was carried out by using standard solutions supplied by Agilent (No. G1820-60410). Multipoint, matrix-matched calibration was performed using a certified calibration standard (Inorganic Ventures IV-ICPMS-71A). The 99.996% purity argon and 99.999% purity helium gas used was purchased from Messer Hungarogáz (Hungary). ICP-MS data processing was performed within the Agilent Mass Hunter (Santa Clara, California, USA) software.

Particular attention was paid to avoid zinc trace impurities during analysis. All labware (polyethylene autosampler vials, certified polymethylpentene volumetric flasks, etc.) were thoroughly cleaned prior to use with dilute ultra-trace quality nitric acid (VWR Chemicals, Pennsylvania, USA), the same as the one used in the preparation of calibration solutions and for the digestion of the proteins, and dried in an ultra high efficiency particulate air filtered environment in a laminar flow hood (Alpine K700). Trace-quality de-ionized labwater from a Merck MilliPore Elix 10 equipped with a Synergy polishing unit (Darmstadt, Germany) was used for preparing all solutions.

2.6. Mass spectrometric investigation of metal ion binding of the KGNK-6 × His protein

Intact protein analysis was performed by mass spectrometry (MS) on an Orbitrap Elite™ (Thermo Scientific) Hybrid Ion Trap-Orbitrap Mass Spectrometer coupled with a TriVersa NanoMate (Advion) chip-based electrospray ion (ESI) source. Prior to ESI-MS measurements, we performed buffer exchange on the protein to 10 mM NH_4HCO_3 pH 8.0 buffer using Amicon Ultra 0.5 mL centrifugal filters with 3 kDa molecular weight cut-off. The protein concentrations during the measurements were 10 μM, as determined based on UV molar absorbances at 280 and 205 nm (Supplementary S1.2). All the masses were measured in the Orbitrap mass analyzer in positive ion mode with 120 k resolution (R = 120,000 at 400 m/z). Protein intact masses (single protonated forms) were determined by deconvolution using the Freestyle 1.6 software tool (Thermo Scientific).

2.7. Catalytic activity assays

BL21 (DE3) *E. coli* cells were transformed by different KGNK and NColE7 plasmids with and without a 6-His affinity tag and incubated at 37 °C overnight in order to check the effect of His tag removal on the bacterial growth.

pUC-EGFP (EGFP stands for the enhanced green fluorescence protein, the gene of which is included in pUC-EGFP) plasmid was applied for DNA cleavage studies by NColE7, KGNK and KGNK-6 × His proteins separately. The KGNK-6 × His protein concentration was kept at 2.8 μM in the catalytic experiments. The DNA cleavage was performed in the absence and presence of Zn^{2+} ions at various metal-to-protein molar ratios from 0:1 to 10:1 to follow the effect of the metal ion on the catalytic activity. The reaction mixtures were incubated at 37 °C for 2 h and the catalytic reaction was stopped by adding SDS to a 1% (m/V) final concentration. Then the DNA cleavage was checked by loading the samples onto 1% (m/V) agarose gel, containing ethidium bromide for visualization of the DNA. Electrophoresis was performed in Tris/acetate/ethylenediaminetetraacetic acid (EDTA) buffer (40 mM Tris, 20 mM acetic acid, and 1 mM EDTA, pH 8.0) using Bio-Rad Wide Mini Sub CellVR GT applying 7 V/cm potential gradient. Gene Ruler 1 kb Plus DNA Ladder (Thermo Scientific) was also applied for comparison.

3. Results and discussion

3.1. DNA cloning and cytotoxicity experiments reflecting the catalytic activity of the nucleases

Colicin E7 metallonuclease is used by *E. coli* to kill competing bacteria under stress conditions. The N-terminal nuclease domain (NColE7) enters the target cell and cleaves the chromosomal DNA non-specifically, resulting in its cytotoxicity. The extremely high catalytic activity of NColE7 is demonstrated by the fact that a single enzyme molecule can kill the cell [45,46]. For this reason, the gene of the NColE7 metallonuclease cannot be cloned into commercial DNA vectors without the simultaneous cloning of the gene of its inhibitory protein Im7 [40,47]. The minor leakage in the protein expression regulation of the plasmids prevents bacterial survival, i.e. growth of colonies. Thus, transformation of bacteria by DNA vectors and subsequent monitoring of the colony growth on LB(amp+) agar plates provides information about the nuclease mediated non-specific DNA cleavage within the cells by the minute amounts of the protein expressed from the inserted gene. Since the Zn^{2+} ion in the catalytic center is essential for the nuclease activity, an important conclusion can also be drawn about the metal ion binding ability of the enzyme or its mutants within the cells.

Recently, we have designed the new pET-21a*-SRHS carrier DNA vector for protein purification by affinity chromatography on Ni(II)-NTA resin. As a result of the protein expression from this vector, a C-terminal hexahistidine peptide tag is fused to the target protein [1]. After inserting the genes of NColE7 and KGNK proteins into this vector and transforming the bacterial cells with these newly created pET-21a*-NColE7-SRHS and pET-21a*-KGNK-SRHS plasmids, bacterial colonies appeared on the LB(amp+) agar plates. This suggests that the modified 6 × His tagged proteins show decreased catalytic activity compared to NColE7 and KGNK, respectively. However, the absence of Im7 gene during the cloning procedure enhances the selection of plasmids including erroneous genes, which results in expressing non-toxic proteins. Therefore, we have checked the nucleotide sequences of the cloned genes. We could obtain the pET-21a*-NColE7-SRHS plasmid with the error-free gene, expressing the expected NColE7-6 × His protein, supporting the decreased catalytic activity. Nevertheless, the sequencing experiments also revealed several pET-21a*-NColE7-SRHS plasmid preparations containing wrong, randomly mutated NColE7 genes, from which modified proteins with decreased or no toxicity could be expressed. The NColE7 nuclease sequence suffered from either random point mutation or random mutation causing a reading frame shift (Table 1). It is worth mentioning that some of the mutations occurred at the same locations detected in our previous article [48], such as the point mutation at D557 or frame shift at …IDIHRGK… amino acid sequence, the latter mutation affecting the H573 residue, essential for the metal ion binding. At the same time the sequences of the verified pET-21a*-KGNK-SRHS plasmids were in agreement with the expected

Table 1
Mutations found in the gene of NColE7 in the DNA cloning experiments.

Types of mutations	Mutation site
Single point mutation	S504L
	D557G
Reading frame shift	…IDIHRGK → …MIFTEVN…
	…PGKA… → …ATLStop
	…RKKFWE… → …VRNSGK…
	…FDDFR… → …LMILStop

sequence. Thus the cytotoxicity of the KGNK-6 × His protein seems to be negligible compared to that of NColE7-6 × His.

After the identification of the pET-21a*-NColE7-SRHS and pET-21a*-KGNK-SRHS plasmids containing the expected sequences, we have applied these DNA constructs for the transformation of various bacterial cells in order to study the influence of the affinity tag on the catalytic activity of the target metallonucleases. These experiments are described in detail in the chapter S1.3 and Fig. S1 in the Supplementary material. The results reflect that the inhibition effect of the 6 × His tag is more pronounced on the less active KGNK nuclease than on NColE7 in agreement with the discussion above.

The Zn^{2+} ion in the active center of NColE7 has an essential role in the catalytic mechanism. The scissile phosphodiester group of the substrate can bind to the metal ion at the fourth coordination site, replacing the coordinated water molecule. Any additional histidine within the C-terminal tag can influence this event. To monitor the possible role of these histidines we have carried out mutation experiments. First, we changed the code of histidine within the SRHS sequence to the code of glutamine (Q) resulting in pET-21a*-NColE7-SRQS and pET-21a*-KGNK-SRQS plasmids. The sequencing results revealed that the mutation of histidine of SRHS was successful in both plasmids, but we could also detect random mutations in some of the pET-21a*-NColE7-SRQS plasmids. Thus, the cytotoxicity of these plasmids in Mach1 and DH5α bacterial cells did not show significant change as compared to the pET-21a*-NColE7-SRHS and pET-21a*-KGNK-SRHS plasmids (data not shown).

The hexahistidine tag is expected to inhibit the catalytic reaction when it binds to the catalytic Zn^{2+} ion. We modified the NColE7-SRQS and KGNK-SRQS proteins by either inserting a stop codon before the 6 × His tag or changing the His tag sequence by a frame shift mutation, but keeping the length of the protein (see detailed description in the chapter S1.3, Scheme S1 and Fig. S2). Both modifications prevent the expression of the inhibitory 6 × His sequence. Therefore, we expected an increased catalytic activity and cytotoxicity of the new plasmids. Fig. 1 shows the comparison of the effect of pET-21a*-Nucl-SRHS, pET-21a*-Nucl-SRQS and pET-21a*-Nucl-SRQS-NoHistag plasmids (where Nucl is either NColE7 or KGNK) on the bacterial colony formation with BL21 cells optimized for protein expression. All the NColE7 containing plasmids killed the cells, but for all KGNK plasmids colony formation was observed. The latter result suggests that the C-terminal tag (even without bearing strongly coordinating amino acid residues) can decrease the catalytic activity of KGNK through a non-specific steric effect, likely involving non covalent interactions with the active site, too.

Multiple explanations can account for these observations: (i) The cooperative action of the N- and C-termini is required for NColE7 to hydrolyze DNA. This kind of intramolecular allosteric activation mechanism may be sterically hindered by the C-terminal protein tag. This phenomenon would allow the fine tuning of the enzyme by optimizing the length of the affinity tag. The tagged enzyme can also be activated by the tag removal from the protein via an optimally positioned hydrolytically sensitive amino acid sequence either by using a specific protease or by Ni(II)-induced cleavage. (ii) The metal ion containing active center at the C-terminus of NColE7 is close enough to the hexahistidine sequence to allow the coordination of this motif to the free site of the catalytic Zn^{2+} ion. This event would also inhibit the nuclease action, as it prevents the metal ion coordination to the scissile phosphodiester group, which is an essential step of the DNA cleavage. In such a mechanism of inhibition the enzyme could be reactivated by the addition of metal ions, which can effectively compete with Zn(II) for the hexahistidine binding site, but do not replace Zn(II) in the active center. (iii) Furthermore, the hexahistidine tag may also form a ternary complex with Zn^{2+} ions including the H545 residue, which is responsible for the formation of the nucleophilic attacking hydroxide in the catalytic reaction.

The inhibition most probably occurs through a complex mechanism, involving the combination of the above eventualities. A further relevant observation is that the inhibitory effect decreases the toxicity to an extent, which is enough for protein expressing bacteria harboring the KGNK-type plasmids to survive, but not for those transformed by the more active NColE7-type plasmids.

3.2. Characterization of the purified protein by CD and ICP MS measurements

Based on the above considerations we purified the KGNK-6 × His protein as described in the Experimental section for further in vitro catalytic experiments to learn more about the effect of His-tag on the enzyme function. The results of the purification procedure are detailed in chapter S1.4 of the Supplementary material. It is worth mentioning that the yield of the pure KGNK-6 × His protein was ~0.3 mg from 1 L culture, i.e. from ~4.0 g of wet cells which is at least 10 times less than the yield we could achieve with e.g. the catalytically inactive ΔN4-NColE7-6 × His protein previously [1]. This reflects that the 6 × His attachment couldn't completely inhibit the nuclease activity of the KGNK protein and the expressed protein is slightly toxic to the cells.

CD spectroscopy was applied to monitor the protein folding after purification and to estimate the fractions of secondary structure elements. Evaluation of the CD spectrum of the KGNK-6 × His protein by the BeStSel software [49] revealed that the relative α-helical content is ~14% (Fig. 2). As expected, this is slightly less than the α-helical content of the Zn^{2+}-loaded KGNK protein calculated by BeStSel: ~16% [42,50]. The reason for this is that KGNK-6 × His is longer by 16 amino acids due to its C-terminal fusion tag, displaying most probably non-helical structure. This result suggests that the protein is in its functionally folded form.

ICP-MS measurements with the same batch of the purified KGNK-6 × His revealed that the protein was obtained in its Zn^{2+}-loaded form containing approximately one equivalent of metal ion (Table S1). Since Zn^{2+} ions in the nuclease domains of Colicin E7 and Colicin E9 proteins are bound extremely tightly in the HNH catalytic center, characterized by an apparent dissociation constant K_d ~10^{-9} value [51,52], we propose that the initially bound metal ion should be in the primary metal ion-binding site in KGNK-6 × His, as well. The KGNK and NColE7 proteins were purified without metal ion, since the removal of the Im7 immunity protein under acidic conditions resulted in the loss of the Zn^{2+} ions, too [42].

3.3. DNA cleavage experiments with the KGNK-6 × His protein

The cleavage of a randomly selected pUC-EGFP plasmid by the KGNK-6 × His enzyme was monitored by agarose gel electrophoresis in the presence of various amounts of Zn^{2+} ions. Upon single-strand cleavage the most compact supercoiled (sc.) form of the plasmid was turned into open circular (oc.) form, while double-strand cleavage (occurring due to the accumulation of single strand DNA cleavage products) resulted in the linear (lin.) form of the plasmid. Further double strand cleavages fractionate the linear DNA into small fragments of various size resulting in a smear on the agarose gel. As it is shown in Fig. 3, the purified KGNK-6 × His protein has a moderate nuclease activity. The band of the supercoiled form of the plasmid starts to decrease in intensity, while the band related to the linear form also

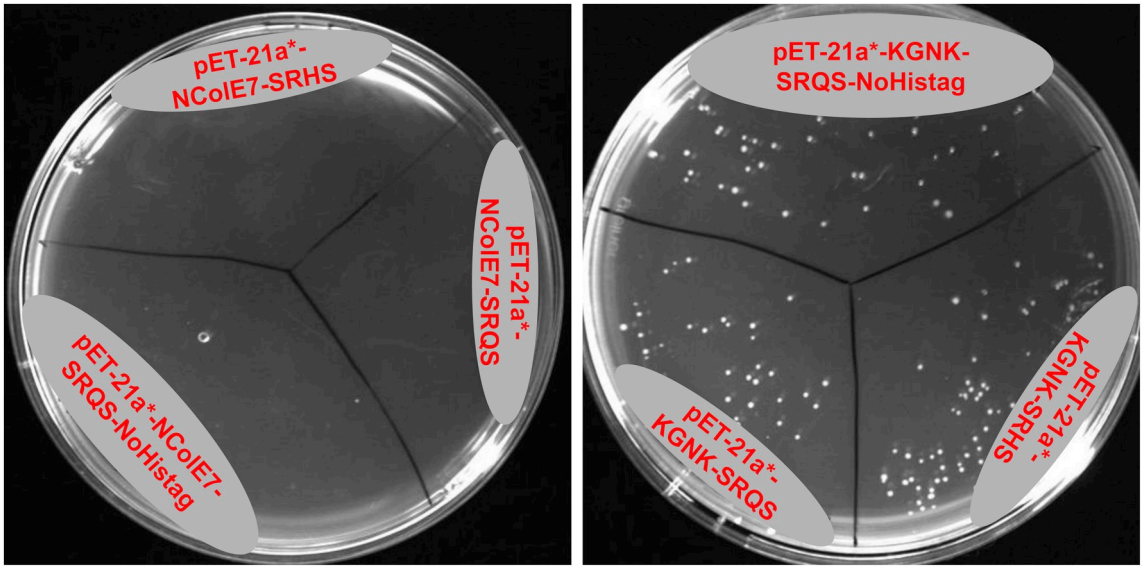

Fig. 1. Inhibition effect of pET-21a*-Nucl-SRHS, pET-21a*-Nucl-SRQS and pET-21a*-Nucl-SRQS-NoHistag plasmids (where Nucl is NColE7 – **left** – or KGNK – **right**) on BL21(DE3) bacterial colony formation with and without His affinity tag. There is no colony formation when Nucl = NColE7, but a few bacterial colonies appeared when Nucl = KGNK.

appears. By adding Zn^{2+} ions to the reaction mixture in increasing amounts we could observe an increase in the catalytic activity from a ~1:2 protein-to-Zn^{2+} molar ratio. The maximum of the DNA cleavage activity was achieved between ~1:3 and 1:5 protein-to-Zn^{2+} molar ratio. Under these conditions, the band of the supercoiled form completely disappears at 60 min; even the band related to the open circular form shows a decreased intensity and smearing of the band of the linear form occurs as a result of the fragmentation due to efficient catalytic process. After a further increase of the metal ion concentration, at 1:10 protein-to-Zn^{2+} molar ratio, the catalytic activity started to decline again.

These results are in agreement with the observation that the catalytic activity of the KGNK-6 × His protein is decreased compared to the KGNK protein (see Fig. S3 for comparison), due to the inhibition effect of the C-terminal tag. However, the increase of the DNA cleavage ability of the enzyme upon increasing metal ion-to-protein ratio suggests that the added metal ion can compete for the 6 × His sequence, which originally may bind to the free site of the catalytic Zn^{2+} ion (Scheme 2) accounting for the coordinative inhibition. Thus, by binding to the 6 × His sequence, the added metal ion enhances the catalytic activity. By saturating the histidines outside the catalytic center with one or two Zn^{2+} ions H545 may also be metallated on further addition of metal ion, preventing the generation of the OH^- nucleophile by the side-chain of this histidine residue. The higher is the metal ion excess the higher is the probability of this type of coordination. This would cause the decrease of the catalytic activity under such conditions. It cannot be excluded that the second or third metal ion, which most probably bind to the hexahistidine sequence, may also coordinate to H545, but the extensive formation of such complex would result in inhibition of the enzyme instead of the activation as observed in the catalytic experiments.

3.4. Mass spectrometric analysis of the metal ion binding properties of the KGNK-6 × His

ESI-MS experiments were carried out to verify the feasibility of the hypothesis described in Scheme 2*a* concerning the formation of mono and oligonuclear complexes of KGNK-6 × His. The experiments were

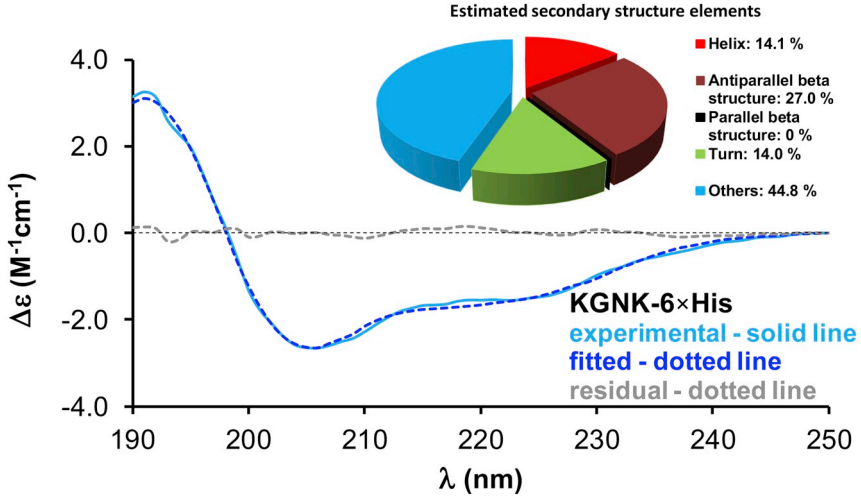

Fig. 2. Fitting of the far UV CD spectra of the KGNK-6 × His protein between 190 and 250 nm for determining the secondary structure fractions by the BeStSel program. The result of the secondary structure estimation is shown in the inset.

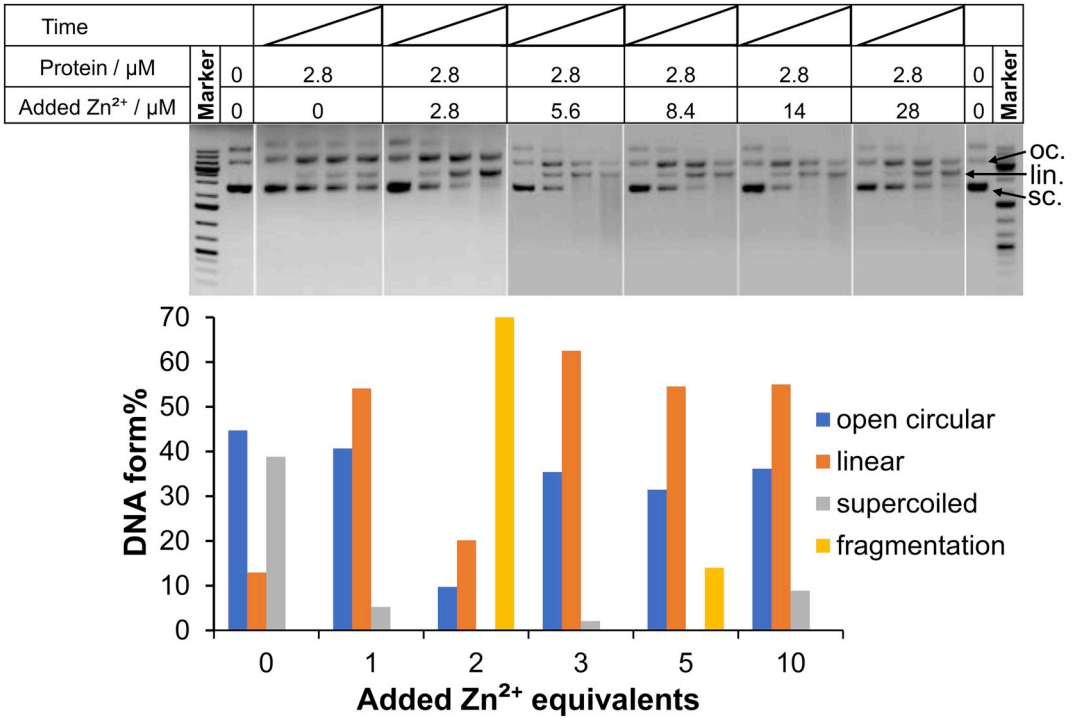

Fig. 3. Top: Agarose gel electrophoresis images showing the cleavage of pUC-EGFP (74 μM for nucleotide pairs) by 2.8 μM KGNK-6 × His protein containing increasing amounts of Zn^{2+} ions. Each column in one experiment represents the catalytic activity after 0, 15, 60, 120 min, from left to right. Gene Ruler 1 kb Plus DNA Ladder (Thermo Scientific) was loaded as a reference, and the untreated pUC-EGFP plasmid for negative control. **Bottom**: Evaluation of the gel pictures by ImageJ program [53,54] for quantitation of the various forms of DNA.

executed by gradually increasing the concentration of the metal ion up to ~4 equivalents of Zn^{2+} relative to the protein. The results of the measurements are presented in Fig. 4. As the ICP-MS measurements indicated, the KGNK-6 × His protein binds approximately one equivalent of Zn^{2+}. The mass spectrum without adding additional metal ion (Fig. 4*a*), shows the presence of the ZnP monocomplex (where P denotes the protein) as the major species, while the Zn_2P complex containing two metal ions also appears.

The mass spectrometric experiments (Fig. 4*a–d*) revealed that the KGNK-6 × His protein is able to bind more metal ions. Up to 6 bound Zn^{2+} ions have been detected by ESI-MS. Based on these measurements the relative amounts of the complexes containing various number of

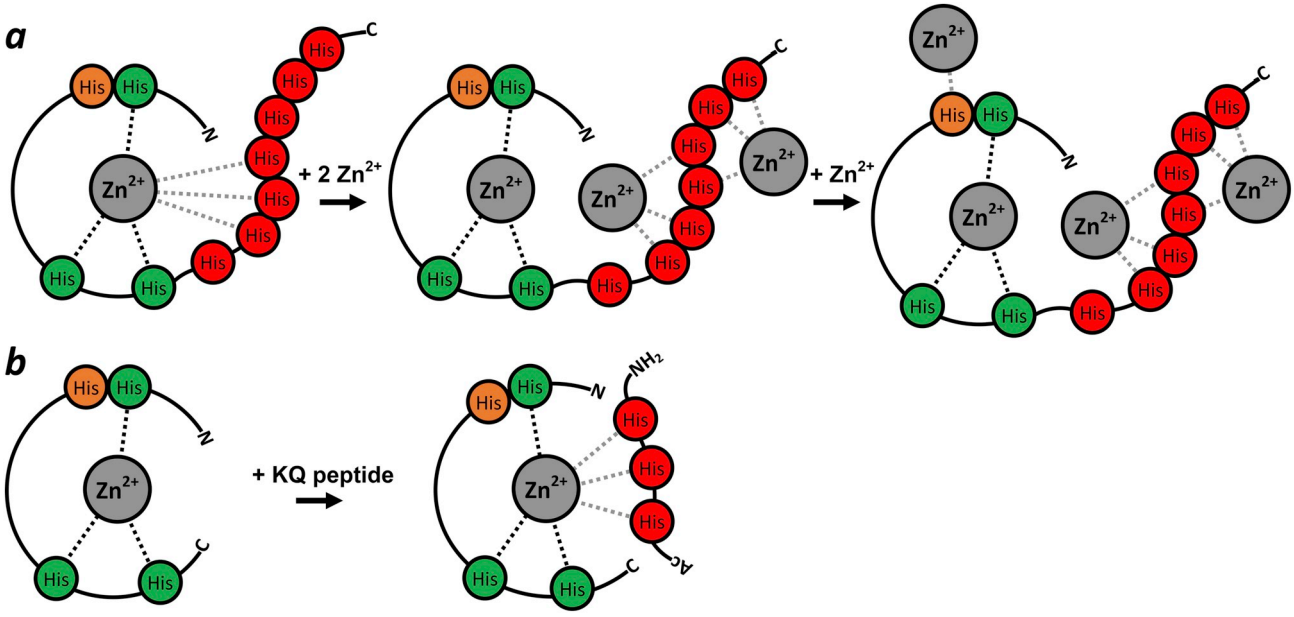

Scheme 2. (*a*) Coordination of histidine residues inside the KGNK-6 × His to an increasing number of Zn^{2+} ions in parallel with the increase of the Zn^{2+}: protein molar ratio. (*b*) Interaction of Zn^{2+} ion, bound to histidines inside the KGNK active center, with an external chelator, such as the KQ peptide (see below) modelling the Zn^{2+}-interaction of the His tag of KGNK-6 × His. The histidines, coordinating to Zn^{2+} ion inside the nuclease active center, are green. H545 is orange, while other histidines outside the native NColE7 sequence are marked red. (In grey scale the histidines coordinating to Zn^{2+} ion inside the nuclease active center are medium, the H545 is light, while other histidines outside the native NColE7 sequence are dark grey.)

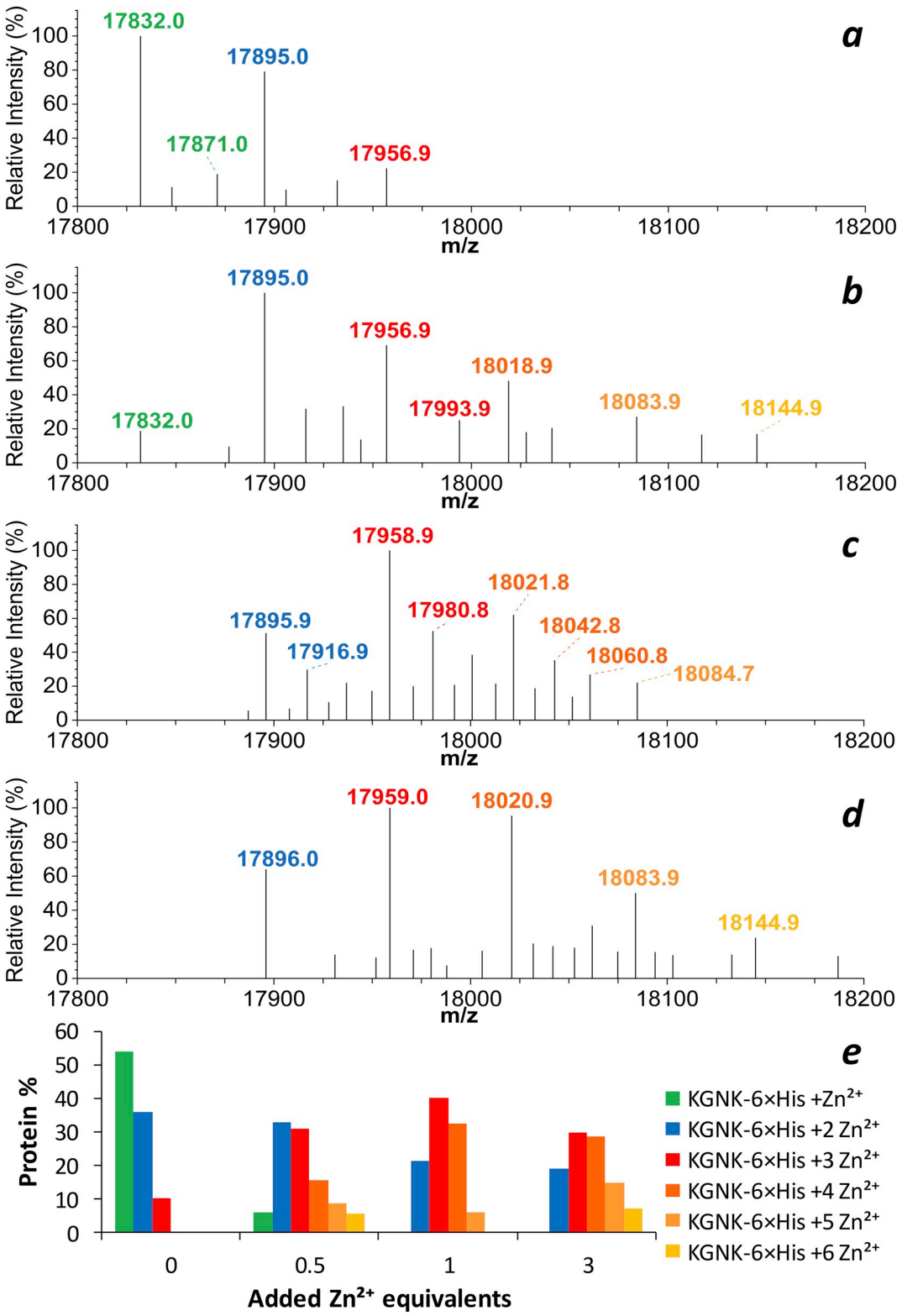

Fig. 4. Deconvoluted monoisotopic MH^+ *m/z* spectra of the KGNK-6 × His protein solution containing increasing amounts of Zn^{2+}. (*a*) The protein solution with approximately 1 equivalent of Zn^{2+}. (*b*), (*c*) and (*d*) after the addition of further 0.5, 1.0 and 3.0 equivalents of Zn^{2+}, respectively. Panel (*e*) shows the estimated relative abundance of the various metal complexes of the protein as a function of the added Zn^{2+} equivalents. Green colour refers to the ZnP (Zn^{2+}: protein = 1: 1) monocomplex; Zn_2P is marked with blue, Zn_3P with red; while the orangish colours refer to the further Zn^{2+} adducts containing more metal ions. (In grey scale the ZnP is medium and Zn_2P is dark grey. Zn_3P is black, while the further Zn^{2+} adducts are light greys.)

metal ions were estimated and plotted versus the added Zn^{2+} equivalents (Fig. 4*e*). For this, we identified the major peaks of the mass spectra in Fig. 4*a–d* and assigned them to the potential Zn^{2+}–KGNK-6 × His species which could be present in the solution (from the monocomplex till the six Zn^{2+} containing adduct). The observed Na^+ and K^+ adducts were also taken into account during the calculations.

The list of the peaks considered for the calculation of the relative abundance diagram is shown in Supplementary Table S2. We summed up the intensities of the peaks belonging to the same species at each titration state and then plotted the percentage of these complexes in Fig. 4*e*. The maximal percentage of the Zn_2P complex of KGNK-6 × His, expected to be catalytically most active, is observed in the presence of ~1.0–2.0 equivalents of Zn^{2+}. Compared to the catalytic activity of the KGNK-6 × His as a function of the Zn^{2+} concentration, this would infer that the Zn_3P species could still be active, while the increasing metal ion concentration results in further coordinated Zn^{2+} ions and inhibition of the nuclease action. Although some of the detected complexes may not form in significant amounts in dilute aqueous solutions and under the conditions applied in the catalytic experiments, these results support the assumption presented in Scheme 2*a* and the clearer interpretation of the catalytic properties of the enzyme, too.

3.5. Modelling the inhibition mechanism of 6 × His in KGNK-6 × His

In order to further examine the type of inhibition by the C-terminal 6 × His tag we investigated the catalytic activity of the NColE7 and KGNK proteins as purified earlier [42], in the presence of metal ion chelators mimicking the coordinative interactions with the Zn^{2+} ion within the active center. The Ac-Lys-His-Pro-His-Pro-His-Gln-NH_2 heptapeptide (further denoted as KQ) containing three histidine residues [55] could not effectively inhibit the activity of the NColE7. NColE7 possesses a very high catalytic activity: it starts to cleave DNA instantly after mixing them together and completely fragmentates the plasmid DNA after 15 min. Under such conditions, the inhibitory effect of the KQ peptide was not observable. However, with KGNK (which has at least 10 times lower activity [42,56]) we could observe the decrease of the DNA cleavage ability as an effect of the presence of the chelator (Fig. S3). The KGNK enzyme causes heavy fragmentation after one hour incubation, while in the presence of 10 equivalents of KQ peptide the linear form is still visible, demonstrating partial inhibition of the catalytic process. This result is consistent with the above experiments in *E. coli* cells showing the extreme activity of NColE7 which could not be completely inhibited even with the hexahistidine sequence attached to the C-terminus, and therefore, it was not possible to express the NColE7-6 × His protein and the other NColE7 containing constructs.

We also carried out similar inhibition experiments with a bis-imidazolyl peptide Gly-BIMA (inset of Fig. 5) able to chelate metal ions through the two imidazole ring nitrogens [57–59]. Applying a decreased nuclease concentration as compared to the experiments with the KQ peptide, the inhibition effect of the peptide was clearly visible even with the NColE7 protein. Mostly the linear form of the DNA was detected after 60 min in the presence of chelator excess, while the NColE7 itself caused heavy DNA fragmentation. The catalytic activity of KGNK was so efficiently inhibited that even the supercoiled form of DNA was still detectable after 60 min in the presence of the competitor (Fig. 5).

One may expect two possible inhibition pathways: the imidazole rings coordinate to the free site of the catalytic Zn^{2+} ion or they remove the Zn^{2+} ion from the active center. Although the Zn^{2+} ion binding affinity of the KQ [55] or Gly-BIMA [57–59] chelators is much smaller than that of the HNH catalytic center, we could not exclude the possibility that the decrease of the catalytic activity is related to competition for the Zn^{2+} ions i.e., the decrease of the concentration of the active catalyst. To better understand the inhibition mechanism, we carried out CD measurements in the presence of the achiral Gly-BIMA. Previously we reported that there is a slight but significant difference in the CD spectra of the apo and holo forms of NColE7 and its mutants [42]. In two separate experiments we added Gly-BIMA and EDTA to the Zn^{2+}-loaded KGNK protein and measured the CD spectra of both solutions (Fig. 6). No change of the protein spectrum was detectable even in the presence of 50 equivalents of the achiral peptide, while EDTA yielded a spectrum identical to that of the apoenzyme. This suggests that the imidazole rings can only bind to the free coordination site of the Zn^{2+} ion inside the catalytic center forming ternary complexes, while the metal ion remains bound to the protein such as it is depicted in Scheme 2*b*. This is a remarkable achievement in elucidating the coordinative inhibitory effect of the 6 × His affinity tag on the metallonuclease activity. A similar modelling of the metal ion affinity tag by an external heptahistidine containing oligopeptide sequence was not successful [13]. The lack of any interference with the enzyme activity suggested only non-specific steric effects of the tag on the TNF proteins [13].

3.6. Influence of the His tag on the structural integrity of KGNK-6 × His

Temperature dependent SRCD measurement series were carried out with NColE7 and KGNK-6 × His proteins in the presence and absence of metal ion with the aim to study the thermal stability of the enzyme. Earlier it was suggested that the removal of the metal ion decreases thermal stability [60]. The results shown in Fig. 7 indicate that the changes in the structure of the enzyme do not occur in a single step.

The first conformational change occurred between 25 and 35 °C and this was significantly affected by the removal of the metal ion from the enzyme. Then the main melting process took place around 49 °C. This probably reflects the conformational change of the central helical

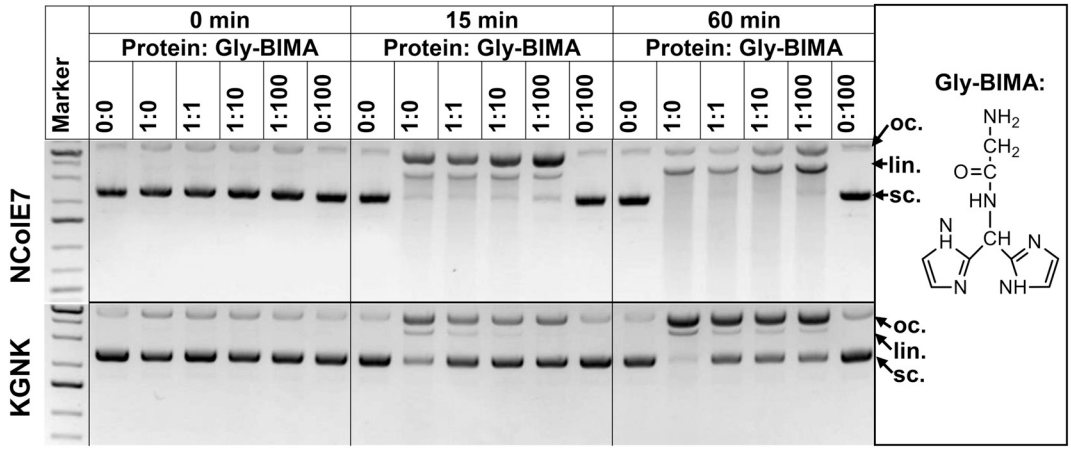

Fig. 5. Digestion of 28 nM pUC-EGFP (75 μM calculated for base pairs) by 0.28 μM NColE7 and 1 μM KGNK in 20 mM HEPES buffer (pH 7.7) in the absence or presence of increasing amounts of Gly-BIMA chelating agent. The samples were kept at 37 °C. The reactions were stopped by 1% (m/V) SDS, freezing and subsequently run on 1% (m/V) agarose gel. Gene Ruler 1 kb Plus DNA Ladder (Thermo Scientific) served as the reference. The inset shows the chemical formula of the Gly-BIMA bis-imidazolyl peptide.

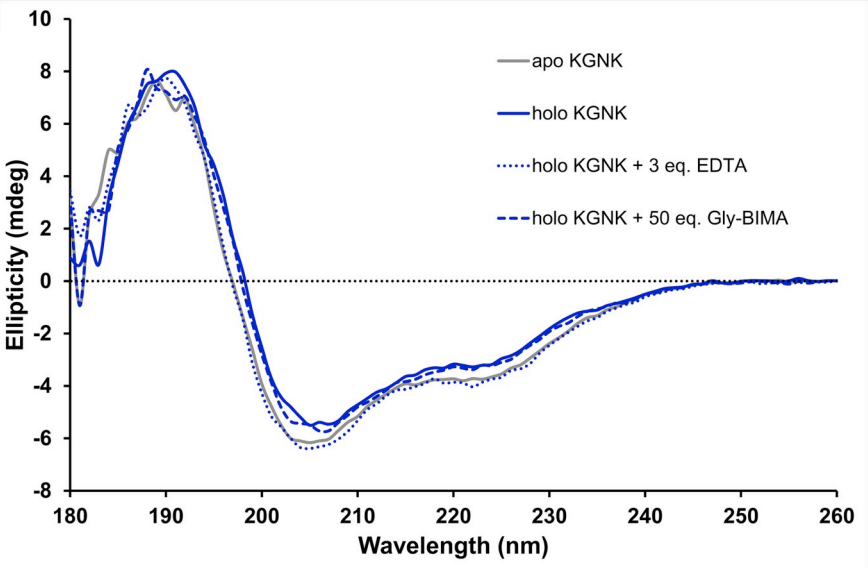

Fig. 6. CD spectra of the KGNK protein in the presence and absence of metal ion and/or various chelators. All spectra were normalized to the same 31.6 μM protein concentration.

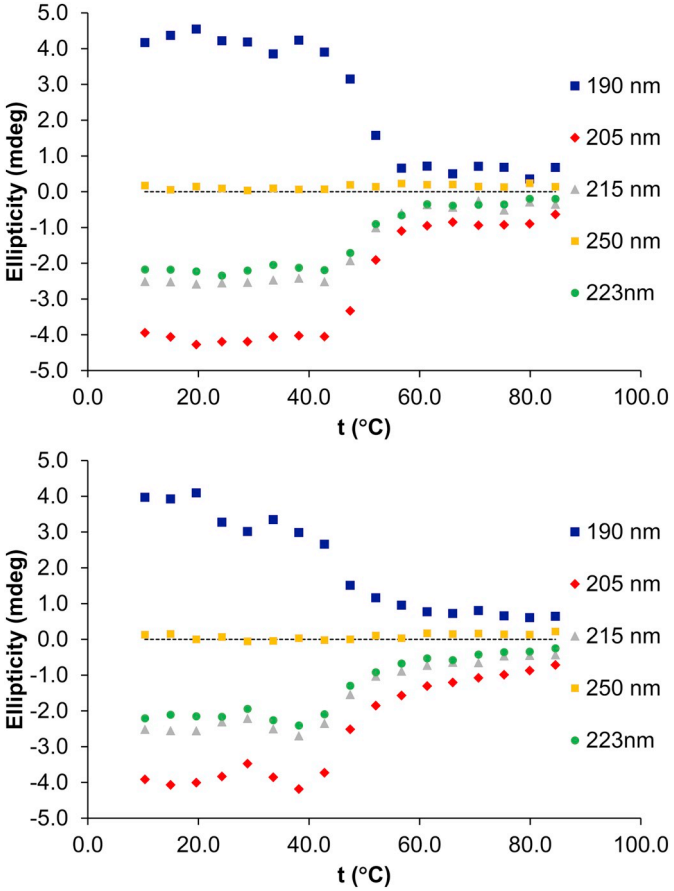

Fig. 7. Temperature dependent SRCD spectra of the Zn^{2+}-loaded (top) and apo (bottom) forms of the KGNK-6 × His protein.

regions of the protein, which is not significantly influenced by the metal ion. For NColE7 the changes occurring between 30 and 40 °C were less pronounced, and the metal ion had only a slight effect (Fig. S4). The curves recorded in the presence of metal ion could be satisfactorily fitted with a single process with a melting point around 50 °C. The main melting process occurred at the same temperature for NColE7 when the metal ion was removed from the catalytic center.

The melting process at low temperature is most probably related to the HNH motif, which might be slightly more flexible and thus, more sensitive to the increasing temperature in the absence of the metal ion. This sensitivity seemed to be more prononounced for the KGNK-6 × His protein. A plausible explanation may be that the C-terminal fusion tag destabilized the interaction between the two termini of NColE7, which is responsible for the stabilization of the structure of the preformed catalytic site [61]. This effect is, however, influenced by the metal ion, suggesting that the coordinated His tag has a negligible disturbing effect on the structure of the HNH motif. This also supports the above observations, that the complex effect of the 6 × His sequence involves steric hindrance, but it also inhibits the enzyme activity by binding to the metal ion in the catalytic center.

4. Conclusions

The 6 × His tag, allowing metal ion affinity chromatographic purification, can also influence the properties of proteins. We showed that even the extremely active NColE7 metallonuclease could be partially inhibited by coordinative (involving the Zn^{2+} containing active center) and non-specific steric interactions of 6 × His sequence. Monitoring the cytotoxicity, originating from the non-specific degradation of the bacterial DNA, showed that the Mach1 and DH5α cells with minute protein expression leakage could survive, but BL21(DE3) cells with less regulated protein expression died when transformed with plasmids containing the NColE7 gene. At the same time the cytotoxic effect of the R447G (KGNK) mutant protein could be reduced to a level allowing the expression and purification of the KGNK-6 × His protein.

In vitro catalytic activity experiments with KGNK-6 × His revealed that the addition of Zn^{2+} excess to the holoprotein results in a complex behavior. The rate of DNA cleavage increased up to a metal-to-protein molar ratio of 3–5: 1, while further excess of metal ion caused inhibition of the catalytic process. The first phenomenon can most probably be explained by the competition of the Zn^{2+} excess for the 6 × His sequence, thereby deliberating this motif from the catalytic Zn^{2+} site. This would result in the activation of the enzyme. In high excess, however, Zn^{2+} may also coordinate to the H545 residue, which has an essential role in the DNA hydrolysis via generating the nuclephylic OH^-. We attempted to simulate these complex formation processes by estimating and refining the apparent stabilities of the Zn_xP species to

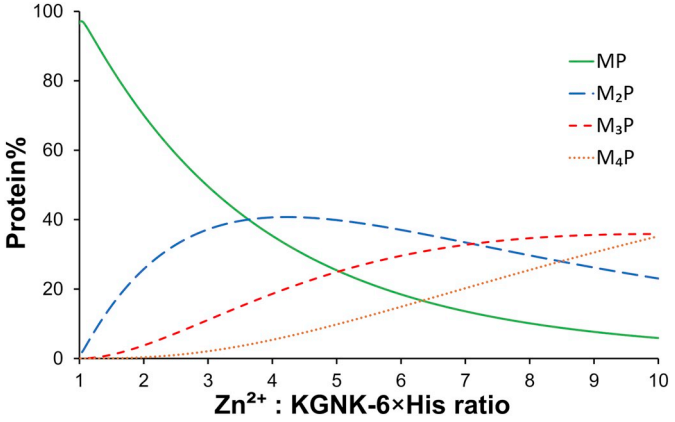

Fig. 8. Calculated species distribution diagram of the Zn^{2+} – KGNK-6 × His (P) system based on the estimated apparent stability constants related to the various metal ion binding sites, as depicted in Scheme 2*a*. c_P = 2.8 μM.

obtain the species distribution best describing the catalytic and MS experiments. Up to four bound metal ions were included considering the number of binding sites potentially offering stability, which is high enough to enable the complex formation in micromolar concentration range. The log*K′* values obtained in this way are ~9.0 for ZnP; ~5.3 for ~Zn_2P; ~4.9 for Zn_3P and ~4.7 for Zn_4P. The first value is in agreement with those published for the Zn^{2+} affinity towards the HNH active center [51,52]. The values for Zn_2P and Zn_3P are consistent with Zn^{2+} coordination towards the oligohistidine peptides binding one or two metal ions [29,55,62]. The hypothetical distribution diagram (Fig. 8) shows that the formation of Zn_4P species becomes significant at > 5 fold Zn^{2+} excess. Since under such conditions the inhibition of the DNA hydrolysis can be observed in accordance with the literature data on NColE7 itself [63], we suppose that the coordination site in Zn_4P is most probably the H545 residue. Taking this into account, the stability related to the binding of the fourth metal ion is fairly high. An explanation of this could be a stability enhancing effect of further amino acid side-chains available for metal ion binding together with H545.

These considerations, well supported by the ESI-MS results (see the distribution diagram for the MS conditions in Supplementary Fig. S5), may help to better understand the catalytic behavior of the KGNK-6 × His protein in the presence of increasing amounts of Zn^{2+}. Based on this model, the catalytically active species are the Zn_2P and Zn_3P complexes with one or two Zn^{2+} ions bound to the oligohistidine moiety while the metal ion in the active center can catalyze the DNA hydrolysis.

The applied KQ or Gly-BIMA chelators could experimentally model the coordinative inhibitory effect of the 6 × His fusion sequence on the catalytic activity of the investigated metallonucleases, although this effect is less pronounced than that of the covalently attached 6 × His tag. We showed that the affinity tag exerts a non-specific steric inhibitory effect, too. Based on these findings, the catalytic activity of the NColE7 or other similar metalloenzymes can be modulated in multiple manner without changing the core enzyme sequence. By the increase of the concentration of competing metal ions the saturation of the 6 × His tag can be achieved and this may decrease its coordinative inhibition effect. A more drastic action to activate the enzyme could be the removal of the whole inhibitory tag by a specific protease mediated hydrolysis, e.g. by a Ni^{2+} ion-induced peptide bond cleavage. The redesign of the metal binding properties of the C-terminal tag also offers multiple opportunities for the fine tuning of the catalytic activity.

Abbreviations

NColE7 The nuclease domain of the Colicin E7 metalloprotein
KGNK R447G mutant of the NColE7 protein.
*Bsm*BI, *Xho*I, *Afl*II Restriction endonucleases.
BL21 (DE3) Chemically competent *E. coli* cells suitable for protein expression.
CD Circular Dichroism.
Mach 1 and DH5α Chemically competent *E. coli* cells for cloning applications.
HEPES 4-(2-hydroxyethyl)-1-piperazineethanesulfonic acid, commonly used buffer in biochemistry and molecular biology.
6 × His tag A hexahistidine-tag is an amino acid motif in proteins that consists of six subsequent histidine (His) residues. The His-tag makes it possible to purify the protein by Ni(II)-affinity chromatography
IPTG Isopropyl β-D-1-thiogalactopyranoside
KOD-FX DNA polymerase from Toyobo Life Science Department.
SDS-PAGE Sodium Dodecyl Sulphate - Polyacrylamide Gel Electrophoresis.
SRCD Synchrotron Radiation Circular Dichroism
OD Optical Density.
pET-21a Cloning/expression vector carrying a code for C-terminal His•Tag® sequence without an easy tag removal opportunity.
QuikChange™ Site-directed in vitro mutagenesis method.
Tricine-SDS-PAGE A Tricine modified Sodium Dodecyl Sulfate - Polyacrylamide Gel Electrophoresis method for protein separation.
Tris Tris(hydroxymethyl)aminomethane, commonly used buffer in biochemistry and molecular biology.

Declaration of competing interest

The authors declare that they have no known competing financial interests or personal relationships that could have appeared to influence the work reported in this paper.

Acknowledgements

This work was supported by the Hungarian National Research, Development and Innovation Office (GINOP-2.3.2-15-2016-00038 and NKFIH K_16/120130), from the Hungarian Academy of Sciences and Japan Society for the Promotion of Science (JSPS), and CALIPSOplus (EU Framework Programme for Research and Innovation HORIZON 2020, grant no. 730872). The authors gratefully acknowledge Katalin Várnagy (University of Debrecen) for providing the BIMA chelator for catalytic experiments. H.A. is a Stipendium Hungaricum PhD fellow supported also by Cultural Affairs & Mission Sector in Egypt. B.H. got a fellowship within the frame of UNKP-19-3 New National Excellence Program of the Ministry of Human Capacities.

Appendix A. Supplementary data

Supplementary data to this article can be found online at https://doi.org/10.1016/j.jinorgbio.2020.111013.

References

[1] H.A.H. Abd Elhameed, B. Hajdu, R.K. Balogh, E. Hermann, É. Hunyadi-Gulyás, B. Gyurcsik, Protein Expr. Purif. 159 (2019) 53–59.
[2] M. Mylonas, A. Krezel, J.C. Plakatouras, N. Hadjiliadis, W. Bal, Chem. Soc., Dalton Trans. (2002) 4296–4306.
[3] A. Krezel, E. Kopera, A.M. Protas, J. Poznanski, A. Wysłouch-Cieszynska, W. Bal, J. Am. Chem. Soc. 132 (2010) 3355–3366.
[4] E. Kopera, A. Krezel, A.M. Protas, A. Belczyk, A. Bonna, A. Wyslouch-Cieszynska, J. Poznanski, W. Bal, Inorg. Chem. 49 (2010) 6636–6645.
[5] A.M. Protas, H.H.N. Ariani, A. Bonna, A. Polkowska-Nowakowska, J. Poznanski, W. Bal, J. Inorg. Biochem. 127 (2013) 99–106.
[6] E.I. Podobas, A. Bonna, J. Inorg. Biochem. 136 (2014) 107–114.
[7] A. Belczyk-Ciesielska, B. Csipak, B. Hajdu, A. Sparavier, M.N. Asaka, K. Nagata, B. Gyurcsik, W. Bal, Metallomics 10 (2018) 1089–1098.
[8] E. Kopera, A. Belczyk, W. Bal, PLoS One 7 (2012) e36350.
[9] E. Kopera, S. Krzywda, M. Lenarcic Živkovic, A. Dvornyk, B. Kłudkiewicz,

K. Grzelak, I. Zhukov, W. Zagórski-Ostoja, M. Jaskólski, W. Bal, PLoS One 9 (2014) e106936.
[10] N.E. Wezynfeld, T. Fraczyk, W. Bal, Coord. Chem. Rev. 327–328 (2016) 166–187.
[11] M. Carson, D.H. Johnson, H. McDonald, C. Brouillette, L.J. DeLucas, Acta Cryst D63 (2007) 295–301.
[12] M.C. Thielges, J.K. Chung, J.Y. Axup, M.D. Fayer, Biochemistry 50 (2011) 5799–5805.
[13] I. Fonda, M. Kenig, V. Gaberc-Porekar, P. Pristovšek, V. Menart, Sci. World J. 2 (2002) 1312–1325.
[14] A. Freydank, W. Brandt, B. Drager, Proteins Struct. Funct. Bioinformat. 72 (2008) 173–183.
[15] A. Chant, C.M. Kraemer-Pecore, R. Watkin, G.G. Kneale, Protein Expr. Purif. 39 (2005) 152–159.
[16] M. Rumlova, J. Benedikova, R. Cubinkova, I. Pichova, T. Ruml, Protein Expr. Purif. 23 (2001) 75–83.
[17] W.T. Booth, C.R. Schlachter, S. Pote, N. Ussin, N.J. Mank, V. Klapper, L.R. Offermann, C. Tang, B.K. Hurlburt, M. Chruszcz, ACS Omega 3 (2018) 760–768.
[18] S. Junaid, S. Qazi, R. Chew, D.C. Bay, R.J. Turner, EmrE, Biochem. Biophys. Rep. 1 (2015) 22–32.
[19] Y.W. Lin, T.L. Ying, L.F. Liao, J. Mol. Model. 17 (2011) 971–978.
[20] Y. Aslantas, N.B. Surmeli, Bioinorg. Chem. Appl. (2019) 8080697.
[21] J. Klose, N. Wendt, S. Kubald, E. Krause, K. Fechner, M. Beyermann, M. Bienert, R. Rudolph, S. Rothemund, Protein Sci. 13 (2004) 2470–2475.
[22] S.J. Bauman, F.C. Church, J. Biol. Chem. 274 (1999) 34556–34565.
[23] S. Karav, E. Talak, M. Tuncer, A. Ozleyen, Int. J. Agric. Innov. Res. 6 (2017) 460–466.
[24] K.A. Majorek, M.L. Kuhn, M. Chruszcz, W.F. Anderson, W. Minor, Protein Sci. 23 (2014) 1359–1368.
[25] Y. Chen, R. Pasquinelli, M. Ataai, R.R. Koepsel, R.A. Kortes, R.E. Shepherd, Inorg. Chem. 39 (2000) 1180–1186.
[26] L.E. Valenti, C.P. De Pauli, C.E. Giacomelli, J. Inorg. Biochem. 100 (2006) 192–200.
[27] J. Watly, E. Simonovsky, R. Wieczorek, N. Barbosa, Y. Miller, H. Kozlowski, Inorg. Chem. 53 (2014) 6675–6683.
[28] D. Brasili, J. Watly, E. Simonovsky, R. Guerrini, N.A. Barbosa, R. Wieczorek, M. Remelli, H. Kozlowski, Y. Miller, Dalton Trans. 45 (2016) 5629–5639.
[29] J. Watły, A. Hecel, M. Rowinska-Zyrek, H. Kozłowski, Inorg. Chim. Acta 472 (2018) 119–126.
[30] R. Waibel, R. Alberto, J. Willuda, R. Finnern, R. Schibli, A. Stichelberger, A. Egli, U. Abram, J. Mach, A. Plückthun, P.A. Schubiger, Nat. Biotechnol. 9 (1999) 897–901.
[31] R. Tavaré, J. Williams, K. Howland, P.J. Blower, G.E.D. Mullen, J. Inorg. Biochem. 114 (2012) 24–27.
[32] C.J. Ackerson, R.D. Powell, J.F. Hainfeld, Methods Enzymol. 481 (2010) 195–230.
[33] D.E. Prasuhn, J.B. Blanco-Canosa, G.J. Vora, J.B. Delehanty, K. Susumu, B.C. Mei, P.E. Dawson, I.L. Medintz, ACS Nano 1 (2010) 267–278.
[34] S. Lata, J. Piehler, Nat. Protoc. 4 (2006) 2104–2109.
[35] A.K. Udit, S. Brown, M.M. Baksh, M.G. Finn, J. Inorg. Biochem. 102 (2008) 2142–2146.
[36] D. Zhao, Z. Huang, Bioinorg. Chem. Appl. (2016) 243–368.
[37] L. Schoonen, K.S. van Esterik, C. Zhang, R.V. Ulijn, R.J.M. Nolte, J.C.M. van Hest, Sci. Rep. 7 (2017) 14772.
[38] A.B. Mason, Q.Y. He, P.J. Halbrooks, S.J. Everse, D.R. Gumerov, I.A. Kaltashov, V.C. Smith, J. Hewitt, R.T.A. MacGillivray, Biochemistry 41 (2002) 9448–9454.
[39] G. Bertani, J. Bacteriol. 186 (2004) 595–600.
[40] M. Sui, L. Tsai, K. Hsia, L. Doudeva, W. Ku, G. Han, H. Yuan, Protein Sci. 11 (2002) 2947–2957.
[41] H. Schägger, Tricine-SDS-PAGE, Nat. Protoc. 1 (2006) 16–22.
[42] E. Németh, T. Körtvélyesi, P.W. Thulstrup, H.E. Christensen, M. Kožíšek, K. Nagata, A. Czene, B. Gyurcsik, Protein Sci. 23 (2014) 1113–1122.
[43] A.J. Miles, S.V. Hoffmann, Y. Tao, R.W. Janes, B.A. Wallace, Spectroscopy 21 (2007) 245–255.
[44] A.J. Miles, R.W. Janes, A. Brown, D.T. Clarke, J.C. Sutherland, Y. Tao, B.A. Wallace, S.V. Hoffmann, J. Synchrotron Radiat. 15 (2008) 420–422.
[45] A.J. Pommer, U.C. Kühlmann, A. Cooper, A.M. Hemmings, G.R. Moore, R. James, C. Kleanthous, J. Biol. Chem. 274 (1999) 27153–27160.
[46] K. Hsia, K. Chak, P. Liang, Y. Cheng, W. Ku, H.S. Yuan, Structure 12 (2004) 205–214.
[47] Y. Cheng, K. Hsia, L.G. Doudeva, K. Chak, H.S. Yuan, J. Mol. Biol. 324 (2002) 227–236.
[48] E. Németh, G.K. Schilli, G. Nagy, C. Hasenhindl, B. Gyurcsik, C. Oostenbrink, J. Comput. Aid. Mol. Des. 28 (2014) 841–850.
[49] A. Micsonai, F. Wien, L. Kernya, Y.-H. Lee, Y. Goto, M. Réfrégiers, J. Kardos, Proc. Natl. Acad. Sci. U. S. A. 112 (2015) E3095–E3103.
[50] E. Németh, R.K. Balogh, K. Borsos, A. Czene, P.W. Thulstrup, B. Gyurcsik, Protein Sci. 25 (2016) 1977–1988.
[51] E.T. van den Bremer, W. Jiskoot, R. James, G.R. Moore, C. Kleanthous, A.J. Heck, C.S. Maier, Protein Sci. 11 (2002) 1738–1752.
[52] L.G. Doudeva, H. Huang, K.C. Hsia, Z. Shi, C.L. Li, Y. Shen, Y.S. Cheng, H.S. Yuan, Protein Sci. 15 (2006) 269–280.
[53] M.D. Abramoff, P.J. Magalhaes, S.J. Ram, Biophoton. Int. 11 (2004) 36–42.
[54] C.A. Schneider, W.S. Rasband, K.W. Eliceiri, Nat. Methods 9 (2012) 671–675.
[55] N.I. Jakab, O. Lőrincz, A. Jancsó, T. Gajda, B. Gyurcsik, Dalton Trans. (2008) 6987–6995.
[56] Z. Shi, K.F. Chak, H.S. Yuan, J. Biol. Chem. 280 (2005) 24663–24668.
[57] O. Szilágyi, K. Ősz, K. Várnagy, D. Sanna, H. Süli-Vargha, I. Sóvágó, G. Micera, Polyhedron 25 (2006) 3173–3182.
[58] K. Ősz, K. Várnagy, H. Süli-Vargha, D. Sanna, G. Micera, I. Sóvágó, Dalton Trans. 10 (2003) 2009–2016.
[59] K. Várnagy, I. Sóvágó, W. Goll, H. Süli-Vargha, G. Micera, D. Sanna, Inorg. Chim. Acta 283 (1998) 233–242.
[60] Y. Lee, C. Lim, J. Mol. Biol. 379 (2008) 545–553.
[61] E. Németh, M. Kožíšek, G.K. Schilli, B. Gyurcsik, J. Inorg. Biochem. 151 (2015) 143–149.
[62] A. Jancsó, A. Kolozsi, B. Gyurcsik, N.V. Nagy, T. Gajda, J. Inorg. Biochem. 103 (2009) 1634–1643.
[63] W.Y. Ku, Y.W. Liu, Y.C. Hsu, C.C. Liao, P.H. Liang, H.S. Yuan, K.F. Chak, Nucl. Acids Res. 30 (2002) 1670–1678.